Effects of discreteness on gauge glass models in two and three dimensions

Satoshi Yotsuyanagi, Yusuke Suemitsu, and Yukiyasu Ozeki
Department of Physics and Chemistry, The University of Electro-Communications, 1-5-1 Chofugaoka, Chofu-shi, Tokyo 182-8585, Japan

(Received 27 November 2008; published 23 April 2009)

The q-state clock gauge glass model is studied to see the effect of discreteness on the Kosterlitz-Thouless (KT) transition and the ferromagnetic (FM) critical phenomenon in random systems. The nonequilibrium relaxation analysis is applied. In two dimensions, the successive transitions of paramagnetic (PM), KT, and FM phases are investigated along the Nishimori line for $q=6$, 8, 10, 12, 14, 16, and 1024 (recognized as ∞) cases. For the upper critical temperature, it is found that the transition temperature is almost the same as in the continuous case for all q values. The lower transition temperature is found to be proportional to $1/q^2$. In three dimensions, the critical behavior of the PM-FM transition is studied along the Nishimori line for $q=6$, 8, 16, and 1024 cases. It is found that the spin discreteness is irrelevant, and the transition belongs to the same universality class as in the (continuous) XY case.

DOI: 10.1103/PhysRevE.79.041138 PACS number(s): 05.70.Jk, 75.10.Nr, 75.40.Mg, 74.81.Fa

I. INTRODUCTION

In the last decades, the physics of frustrated and disordered systems has been one of most fascinating subjects for theorists and experimentalists. The gauge glass (GG) is a typical example in this category and has attracted much attention. It describes thermodynamics of various systems such as disordered magnets with random Dzyaloshinskii-Moriya interaction [1], Josephson-junction arrays with positional disorder in a magnetic field [2], and so on. In the weakly disordered regime in two dimensions (2Ds), there has been a controversy about the existence of reentrant transition from the Kosterlitz-Thouless (KT) phase [3] to non-KT one [1,2,4–15]. With all these studies, the instability of the KT phase against a small disorder has been pointed out by the perturbation expansion and renormalization-group (RG) analysis [16,17], while it is denied by numerical simulations [10,11,14,15] and other analyses [9,11–13,18,19]. In three dimensions (3Ds), the ferromagnetic (FM) phase appears instead of the KT phase, and the spin-glass (SG) transition for strongly disordered regime has been confirmed in the gauge glass systems by numerical simulations [20–23] and RG analyses [24,25], which is consistent with experimental observations [26–28].

In two dimensions for the pure case, the effect of discrete spin state on the KT transition has been investigated by the use of the clock model. José *et al.* [29] pointed out that typical successive transitions of paramagnetic (PM)-KT-FM phases occur when $q \geq 5$. In random case, exact locations of multicritical points are conjectured for the random Z_q models by the use of the duality argument with the replica method [30]. In three dimensions, for the pure Z_n model, an RG analysis has suggested that there exists only one transition for PM-FM phases and the transition type is XY type [31].

In the present paper, we investigate the q-state clock GG models in two and three dimensions. To clarify the effect of the spin discreteness, we investigate the KT-transition temperatures for $q=6$, 8, 10, 12, 14, 16, and 1024 cases in two dimensions and critical exponents for $q=6$, 8, 16, and 1024 cases in three dimension. The Z_q discrete symmetry is imposed into the original GG model, and the effect of discreteness, which would be related to frustration phenomena, is discussed. We find an applicability of the duality equation partly, which is derived for the random Z_q Villain model [30].

The nonequilibrium relaxation (NER) analysis is applied to estimate transition temperatures and critical exponents. The NER method is an efficient numerical technique for analyzing equilibrium phase transition [32]. It provides the critical temperature and critical exponents accurately for second-order transition systems [33–35] and has been used successfully to study various problems, including frustrated and/or random systems [36]. It has also been extended beyond second-order transitions; e.g., the KT transition [35,37,38] and the first-order transition systems [39]. In the NER analysis, the equilibration step is not necessary. Simulation is made only up to steps when the asymptotic behavior indicates the equilibrium state. Thus, one can analyze large systems as compared with equilibrium simulations. This advantage becomes more effective for slow-relaxation systems. Since the method is simple and straightforward, it can be extended to various systems. For the GG model with $q=\infty$, the NER method showed the KT transition along the Nishimori line [40] which reveals the stability of the KT phase against small disorder.

The organization of the paper is as follows. In Sec. II, the clock GG model is introduced, and some previous results are briefly reviewed. In Sec. III, the result in 2D is shown for the analysis of the KT-transition temperatures. The result in 3D is shown in Sec. IV for the analysis of the FM critical behavior. Section V is devoted for remarks.

II. CLOCK GAUGE GLASS MODELS

We consider two kinds of GG models, which have the same symmetry, in two dimensions. The first one that we call the "cosine type" is based on the planar rotator model with random gauge variables. The second one that we call the "Villain type" is defined by a piecewise harmonic interaction

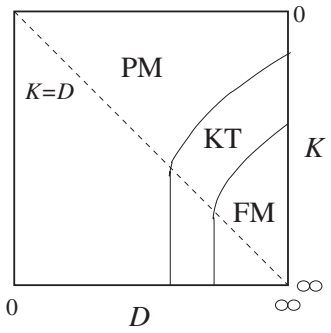

FIG. 1. Expected phase diagram of the q-state clock GG model in two dimensions with $q \geq 5$. The dashed line indicates the Nishimori line ($K=D$).

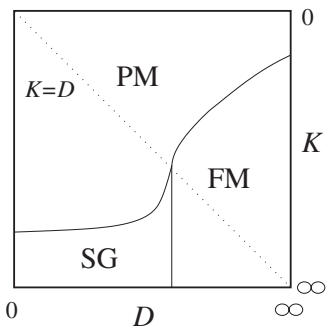

FIG. 2. Expected phase diagram of the q-state clock GG model in three dimensions. The dashed line indicates the Nishimori line ($K=D$).

[41]. The Hamiltonian of the cosine-type model is expressed as

$$\mathcal{H} = -J\sum_{\langle ij\rangle} \cos(\theta_i - \theta_j + A_{ij}), \tag{2.1}$$

where $J>0$, the summation $\langle ij\rangle$ is taken over all nearest-neighboring sites on the square lattice, θ_i is the angle of the rotator spin, and A_{ij} is the random gauge associated with each pair. For the q-state clock case, each spin takes q discrete values as

$$\theta_i \in \left\{ \frac{2\pi n_i}{q} | n_i = 0,1 \cdots q-1 \right\}. \tag{2.2}$$

The quenched random variable A_{ij} takes the same values and obeys the distribution function

$$P(A_{ij}) = \exp(D\cos A_{ij}) / \sum_{\ell'=0}^{q-1} \exp\left(D\cos\frac{2\pi\ell'}{q} \right), \tag{2.3}$$

where D is the parameter controlling the strength of randomness. The pure case is corresponding to $D=\infty$. In the case of $q\to\infty$, the model becomes identical with the (continuous) GG model, which shows the KT transition like the pure XY (planar rotator) model [38]. It is remarkable that for the pure case, the q-state clock model in two dimensions shows typical successive transitions of PM-KT-FM phases when $q \geq 5$ [29]. In the following, we denote that the PM-KT-transition temperature is T_{KT1} and the KT-FM one is T_{KT2} and temperature is measured in units of J/k_B. The expected phase diagram is shown in Fig. 1, where $K=Jk_BT$. For the pure case, it has been clarified by the NER method for the KT transition that the upper transition temperatures T_{KT1} are very close to the continuous case ($q=\infty$) and clock models (finite q's), e.g., $T_{\mathrm{KT1}}=0.894(4)$ for $q=\infty$ and $T_{\mathrm{KT1}}=0.899(5)$ for $q=6$ [38]. For the random case on the Nishimori line ($K=D$) with $q=\infty$, the NER method showed that $T_{\mathrm{KT1}}=0.325(6)$ in cosine type and $T_{\mathrm{KT1}}=0.382(12)$ in Villain-type ($T_{\mathrm{KT2}}=0$ in the continuous case) [40], which reveals the stability of the KT phase against small disorder.

The Nishimori line was originally introduced for the random Ising models [42]. It was extended to other gauge symmetric models including the gauge glass ones [43]. On this line, some exact relations are derived between thermodynamic quantities, which provide a plausible argument that the multicritical point is located on it.

The function (2.3) is chosen so that the model satisfies the gauge theory from which various analytic properties are derived [18,19]. We consider that it behaves similarly to the Gaussian distribution and the difference between them is irrelevant, since the same properties are derived by the gauge theory if one considers the other model, the "Villain-type" GG model. This is defined by the local Boltzmann factor based on the periodic Gaussian potential [41]

$$\exp[-V(\theta_i - \theta_j + A_{ij})] = \sum_{m=-\infty}^{\infty} \exp\left[-\frac{K}{2}(\theta_i - \theta_j + A_{ij} + 2\pi m)^2 \right], \tag{2.4}$$

instead of the Hamiltonian (2.1). The exact location of multicritical points is conjectured for the random Z_q models by the use of the duality argument with the replica method [30]. Let us denote the probability of a local gauge being the lth state as

$$p_\ell(D) \equiv P\left(A_{ij} = \frac{2\pi\ell}{q} \right) = \exp\left(D\cos\frac{2\pi\ell}{q} \right) / \sum_{\ell'=0}^{q-1} \exp\left(D\cos\frac{2\pi\ell'}{q} \right). \tag{2.5}$$

If the double transition occurs as shown in Fig. 1 on $K=D$, the theory yields a condition for two transition points as

$$-\sum_{\ell=0}^{q-1} \{ p_\ell(D_1)\log_q p_\ell(D_1) + p_\ell(D_2)\log_q p_\ell(D_2) \} = 1. \tag{2.6}$$

In three dimensions, we consider only the cosine-type GG model. The expected phase diagram is shown in Fig. 2. The KT phase does not appear and there exists only one transition even for finite q's. For the pure case, this transition has been pointed out in the XY-universality class for any q cases [31].

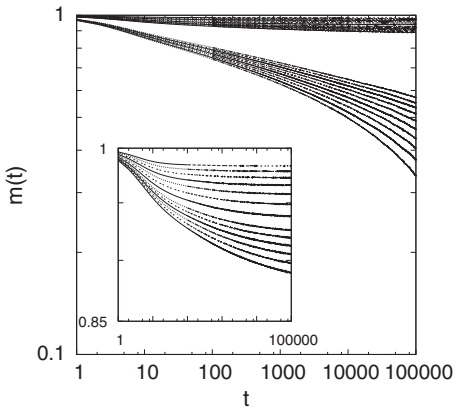

FIG. 3. Relaxation of magnetization $m(t)$ for the Villain-type model with $q=6$ in a double-log plot. For temperatures in $0.21 \leq T \leq 0.28$ and $0.48 \leq T \leq 0.57$, the data are plotted with an interval of $\Delta T=0.01$ and so do in $0.28 \leq T \leq 0.305$ with $\Delta T=0.005$, which are used for the following scaling analysis. The inset is a magnification of data for the low-temperature parts.

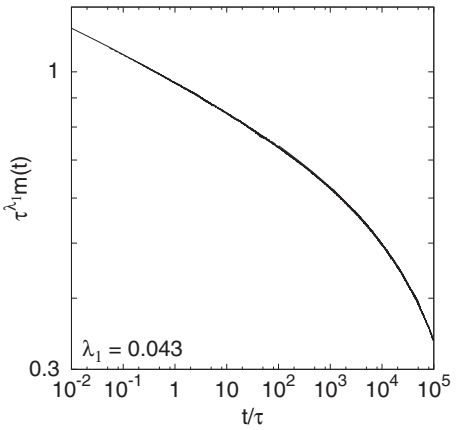

FIG. 4. Scaling plot of $m(t)$ for the $q=6$ case in $0.48 \leq T \leq 0.57$ fitted using Eq. (3.2) with appropriately chosen $\tau(T)$ and $\lambda_1=0.043$.

III. NUMERICAL RESULTS IN TWO DIMENSIONS

Using the NER analysis for KT transitions, we investigate the GG model of both types for $q=6,8,10,12,14,16$ cases along the Nishimori line ($K=D$) where the effect of randomness is observed clearly. Since two transition temperatures are necessary to be distinguished, we perform the scaling analysis for two temperature regimes. In the NER analysis of the KT phase, we choose a complete ordered state ($\theta_i=0$ for all i) as the initial state and calculate the relaxation of magnetization

$$m(t) \equiv \frac{1}{N}\sum_i [\langle \cos\, \theta_i(t)\rangle], \tag{3.1}$$

where $\langle \cdots \rangle$ represents the dynamical average, and $[\cdots]$ is the average for the disorder. We use the skew boundary condition [44] for the purpose of efficient calculations. For each q case, calculations are carried out on a 1001×1000 lattice up to the observation time 10^5 Monte Carlo steps (MCS). About 64 independent runs are performed for the averaging. The size dependence is checked to be negligible up to this observation time, when we compare the data with those on a 801×800 lattice. This reveals that the effect of boundary condition on thermodynamic behaviors is also negligible.

As an example, we show the analysis of the Villain-type model for $q=6$ case. The relaxation of $m(t)$ is plotted in Fig. 3. Let us consider the upper transition temperature T_{KT1}. Similar to the scaling analysis in the equilibrium Monte Carlo simulation, we cannot distinguish the transition point and the KT regime from the relaxation behavior directly, since it always decays in a power law inside the KT phase. It is much different from the NER analysis for the standard second-order-transition systems. Due to the critical relaxation in the KT phase, it is not apparent whether the observed power-law behavior stays in a longer time scale. In fact, in $0.48 \leq T \leq 0.51$ in Fig. 3, which is higher than the expected T_{KT1}, the relaxation behavior almost keeps a power law within the observed time $t=1.5 \times 10^5$. In Fig. 3, one can see a coherent behavior of the relaxation function $m(t)$ in the regime of $0.48 \leq T \leq 0.57$. After the same initial relaxation time which is about 100 MCS, it decays like in a power law up to a finite time τ then a crossover occurs and it changes to decay exponentially. The time scale τ is called the relaxation time depending on the temperature. Therefore, it is natural to expect the scaling form [35] for the PM regime

$$m(t) = \tau^{-\lambda_1} g(t/\tau), \tag{3.2}$$

where λ_1 is the dynamic exponent. We use this scaling form to estimate T_{KT1} precisely from the NER function. First, we estimate $\tau(T)$ at each temperature using the scaling form (3.2). We plot $\tau^{\lambda_1}m$ as a function of t/τ in the double-log scale with independent scaling parameters λ_1 and τ. In this fitting, it is somehow easy to decide the best-fit parameters, since changing the parameter τ causes just the parallel translation of curve. Precisely speaking, since λ_1 is a constant independent of temperature, we first fix λ_1 and estimate τ at each temperature. It is repeated for several values of λ_1. The best value for λ_1 is determined by minimizing the total amount of fitting residual. The result with $\lambda_1=0.043$ is shown in Fig. 4, where the estimated $\tau(T)$ is plotted in Fig. 5. Next, we estimate T_{KT1} from the estimated $\tau(T)$. As T ap-

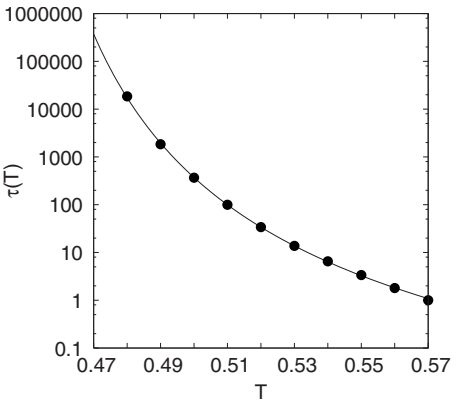

FIG. 5. Relaxation time for $q=6$ case for $T \geq T_{\mathrm{KT1}}$ in units of τ at $T=0.57$. The points fitted to Eq. (3.3) with $T_{\mathrm{KT1}}=0.435$.

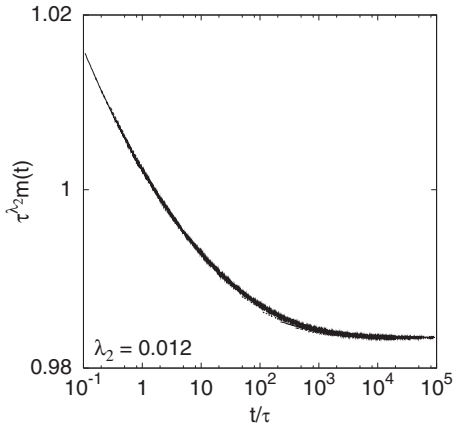

FIG. 6. Scaling plot of $m(t)$ for the $q=6$ case in $0.21 \leq T \leq 0.305$ fitted using Eq. (3.2) with appropriately chosen $\tau(T)$ and $\lambda_2=0.012$.

proaches T_{KT1}, the correlation length diverges exponentially as $\xi \sim \tilde{a} \exp(\tilde{b}/\sqrt{|T-T_{\mathrm{KT1}}|})$ [3,45]. We expect that the relaxation time diverges in the same way,

$$\tau(T) = a \exp(b/\sqrt{|T-T_{\mathrm{KT1}}|}), \tag{3.3}$$

instead of a power-law divergence in standard second-order transitions. This is reasonable if one assumes the relation $\tau \sim \xi^z$ with a definite value of z. Using the χ^2 fitting with parameters a, b, and T_{KT1}, we obtain the best fit as shown in Fig. 5 with $T_{\mathrm{KT1}}=0.435(12)$. Note that the error bar of T_{KT1} (and T_{KT2}) in the present investigation is estimated from the fitting quality of τ like for the plot in Fig. 5. In order to estimate the actual error bars, we have to examine also the fitting quality of the magnetization (Fig. 4), which is a difficult task. This fact has to be especially kept in mind.

A similar analysis can be made for the lower transition point T_{KT2} with T_{KT2} and λ_2 replaced by T_{KT1} and λ_1 in Eqs. (3.2) and (3.3). The scaling fit for the data in $0.21 \leq T \leq 0.305$ is shown in Fig. 6 with $\tau(T)$ plotted in Fig. 7 and $\lambda_2=0.012$. Using the χ^2 fitting Eq. (3.3) with parameters a, b, and T_{KT2}, we obtain the best fit as shown in Fig. 7 with $T_{\mathrm{KT2}}=0.353(27)$.

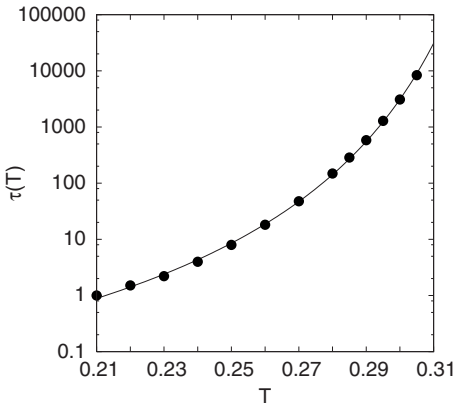

FIG. 7. Relaxation time for $q=6$ case for $T \geq T_{\mathrm{KT2}}$ in units of τ at $T=0.21$. The points fitted to Eq. (3.3) with $T_{\mathrm{KT2}}=0.353$.

TABLE I. Summary of estimated transition temperatures T_{KT1} and T_{KT2} and corresponding dynamical exponents λ_1 and λ_2 for the Villain-type model. The temperature is measured in units of J/k_B. The conjectures from the duality equations are also listed; T_2^D is the lower transition temperature calculated from Eq. (2.6) with the present estimation of T_{KT1} assumed.

q	T_{KT1}	λ_1	T_{KT2}	λ_2	T_2^D
6	0.435(12)	0.043	0.353(27)	0.012	0.357
8	0.434(12)	0.047	0.193(21)	0.007	0.200
10	0.435(16)	0.048	0.134(6)	0.005	0.127
12	0.424(7)	0.046	0.096(5)	0.004	0.090
14	0.421(10)	0.045	0.069(2)	0.003	0.067
16	0.429(10)	0.047	0.050(2)	0.003	0.050
...					
∞	0.429(10)	0.045	0		

For other q cases, we show the results summarized in Table I together with the previously obtained $q=1024$ considered as $q=\infty$ (continuous case). The q-dependence of T_{KT1} and T_{KT2} are shown in Fig. 8. This figure shows that the PM-KT-transition temperatures T_{KT1} are very close ($T \simeq 0.430$) irrespective of q [46] and the KT-FM transition temperatures T_{KT2} are proportional to $1/q^2$. The q-state clock model has the energy discreteness which is impassable in the low temperature. Because it turns out that the energy discreteness depends on $1/q^2$, KT-FM transition temperatures T_{KT2} are also linear $1/q^2$.

The same analysis is applied to the cosine-type model. The relaxation of $m(t)$ for $q=6$ case is plotted in Fig. 9. The scaling plot of the data in $0.37 \leq T \leq 0.45$ fitted to Eq. (3.2) with $\lambda_1=0.042$ is shown in Fig. 10. The fitting to Eq. (3.3) is shown with $T_{\mathrm{KT1}}=0.338(2)$ in Fig. 11. We also estimate $\lambda_2=0.011$ in Fig. 12 and $T_{\mathrm{KT2}}=0.302(5)$ in Fig. 13. The same analysis is made for other q cases. The results are summarized in Table II. The q dependence of T_{KT1} and T_{KT2} is shown in Fig. 14. As observed for the Villain-type case above, for the cosine-type case, we also find that the upper critical temperatures T_{KT1} are very close ($T \simeq 0.320$) to the

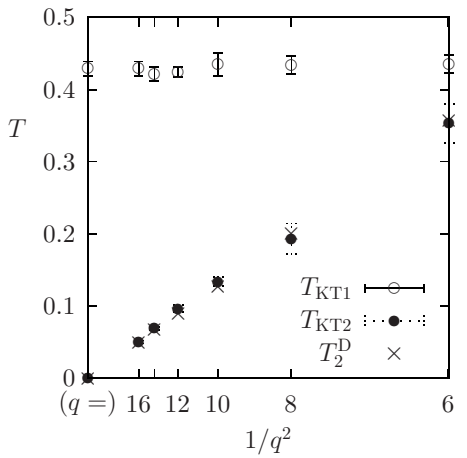

FIG. 8. $1/q^2$ dependence of T_{KT1}, T_{KT2}, and T_2^D for the Villain-type GG model.

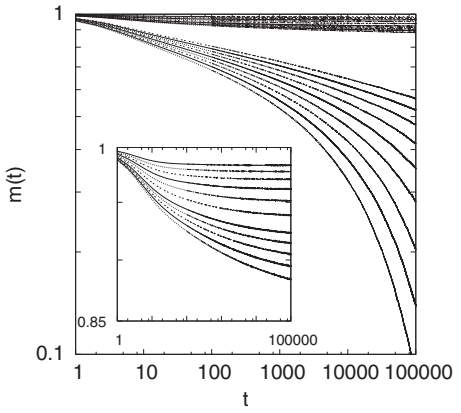

FIG. 9. The relaxation of magnetization $m(t)$ for the cosine-type model with $q=6$ in double-log plot. For temperatures in $0.19 \leq T \leq 0.24$ and $0.37 \leq T \leq 0.45$, the data are plotted with an interval of $\Delta T=0.01$ and so do in $0.24 \leq T \leq 0.27$ with $\Delta T=0.005$, which are used for the following scaling analysis. The inset is a magnification of data for the low-temperature parts.

one in the continuous case, and the lower transition temperatures T_{KT2} are proportional to $1/q^2$.

Next, let us check the duality (2.6). In Table I for the Villain case, we have listed two lower temperatures: the one is T_{KT2} estimated by the NER method and the other is T_2^D calculated from Eq. (2.6) with the presently obtained upper transition temperature T_{KT1} substituted. They are almost identical with each other (see Fig. 8). This indicates the applicability of Eq. (2.6) obtained by the duality theory [30,47,48]. On the other hand, for the cosine-type, for which the results are summarized in Table II, we also calculated the lower transition temperature T_2^D from Eq. (2.6) with the presently obtained upper transition temperature T_{KT1} substituted. They are almost identical with each other too (see Fig. 14). Although the cosine-type model is not self-dual, it suggests that the deviation from the self-duality is irrelevant for the amount of the transition temperature.

IV. NUMERICAL RESULTS IN THREE DIMENSIONS

We analyze the q-state clock GG model in three dimensions for $q=6,8,16$ cases along the Nishimori line ($K=D$). It

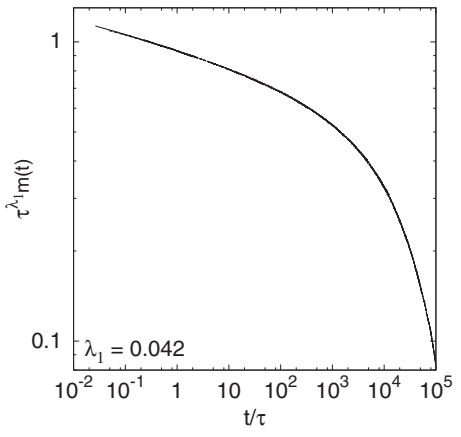

FIG. 10. Scaling plot of $m(t)$ for the $q=6$ case in $0.37 \leq T \leq 0.45$ fitted using Eq. (3.2) with appropriately chosen $\tau(T)$ and $\lambda_1=0.042$.

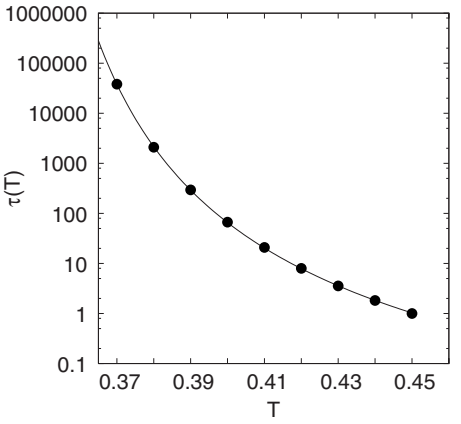

FIG. 11. Relaxation time for $q=6$ case for $T \geq T_{\mathrm{KT1}}$ in units of τ at $T=0.45$. The points fitted to Eq. (3.3) with $T_{\mathrm{KT1}}=0.338$.

is expected that the GG model in three dimensions shows the PM-FM phase transition. We denote T_c as the PM-FM transition temperature. In the NER analysis [32], we choose a complete ordered state ($\theta_i=0$ for all i) as the initial state. We expect that $m(t)$ decays exponentially to zero in the PM phase and so does algebraically at the transition point. In the FM phase, it decays to the spontaneous value m_{eq} exponentially. The asymptotic behavior of magnetization $m(t)$ is summarized as

$$m(t) \sim \begin{cases} \exp(-t/\tau) & (T > T_c), \\ t^{-\lambda_m} & (T = T_c), \\ m_{\mathrm{eq}} & (T < T_c), \end{cases} \tag{4.1}$$

where τ is the relaxation time and λ_m is the dynamical exponent which characterizes the power-law decay of the magnetization at the critical point. To see the asymptotic power-law decay of the NER function $m(t)$ clearly, we usually analyze its logarithmic derivative,

$$\lambda_m(t) \equiv -\frac{\mathrm{d} \log m(t)}{\mathrm{d} \log t}, \tag{4.2}$$

which is practically more convenient. We call it the local exponent [of $m(t)$]. It is noted that the dynamical function

TABLE II. Summary of estimated transition temperatures T_{KT1} and T_{KT2} and corresponding dynamical exponents λ_1 and λ_2 for the cosine-type model. The temperature is measured in units of J/k_B. The conjectures from the duality equations are also listed; T_2^D is the lower transition temperature calculated from Eq. (2.6) with the present estimation of T_{KT1} assumed.

q	T_{KT1}	λ_1	T_{KT2}	λ_2	T_2^D
6	0.338(2)	0.042	0.30(5)	0.011	0.310
8	0.319(8)	0.044	0.187(4)	0.007	0.194
10	0.325(6)	0.046	0.117(4)	0.004	0.126
12	0.321(4)	0.044	0.087(3)	0.003	0.090
14	0.322(5)	0.045	0.068(1)	0.003	0.067
16	0.312(8)	0.042	0.051(2)	0.002	0.053
⋯					
∞	0.322(6)	0.050	0		

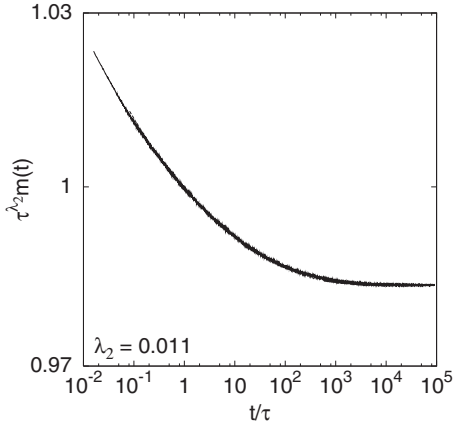

FIG. 12. Scaling plot of $m(t)$ for the $q=6$ case in $0.19 \leq T \leq 0.27$ fitted using Eq. (3.2) with appropriately chosen $\tau(T)$ and $\lambda_1=0.011$.

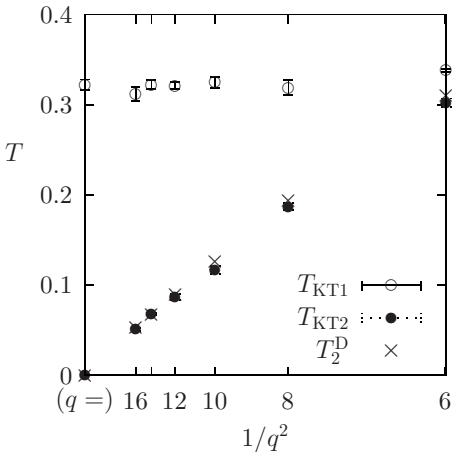

FIG. 14. $1/q^2$ dependence of T_{KT1}, T_{KT2}, and T_2^D for the cosine-type GG model.

$\lambda_m(t)$ should be distinguished from the exponent λ_m which is time independent. We will use the same convention for other exponents. Let us examine three typical behaviors in Eq. (4.1). When t goes to infinity, we obtain the asymptotic behavior

$$\lambda_m(t) \to \begin{cases} \infty & (T > T_c), \\ \lambda_m & (T = T_c), \\ 0 & (T < T_c). \end{cases} \tag{4.3}$$

To estimate the transition temperature T_c, the NER method provides a simple procedure for standard second-order transition cases. In principle, Eq. (4.1) or equivalently Eq. (4.3) which is more practical is used to identify the phase at each temperature.

As an example, we show the NER analysis for the six-state clock GG model in three dimensions. The result is plotted in Fig. 15. Calculations are carried out on a $101 \times 101 \times 100$ lattice up to the observation time $2000 \sim 30\,000$ MCS. About 64 independent runs are performed for averaging in $0.3 \leq T \leq 1.0$ and $512 \sim 2048$ independent runs are performed for averaging in $0.78 \leq T \leq 0.79$. By careful observation, one can find the difference of asymptotic behavior; one is slightly bending up indicating the asymptotic saturation in the FM phase and one is bending down indicating the exponential decay in the PM phase. To estimate more accurate T_c, we plot local exponent $\lambda_m(t)$ versus $1/t$ in Fig. 16. As shown in Eq. (4.3), at the critical point where $m(t)$ decays to zero algebraically, the local exponent $\lambda_m(t)$ approaches a finite value in the limit of $1/t=0$. It is clearly seen in Fig. 16 that the curve turns down at $T=0.783$ for $1/t \to 0$ and turns up at $T=0.787$, which is consistent with the above direct observation for $m(t)$. This provides the estimation of the transition temperature as $T_c=0.785(2)$.

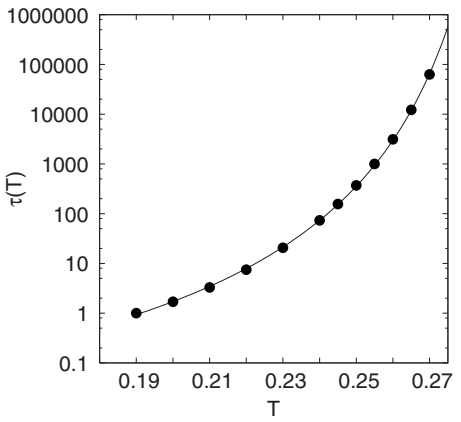

FIG. 13. Relaxation time for $q=6$ case for $T \geq T_{KT2}$ in units of τ at $T=0.19$. The points fitted to Eq. (3.3) with $T_{KT2}=0.302$.

We also estimate the critical exponents. The simulation is performed at the temperature $T_c=0.785$ estimated in Fig. 16. Calculations are carried out on a $51 \times 51 \times 50$ lattice up to the observation time 1000 MCS. About 1.6×10^6 independent runs are used for the statistical averaging. We use the NER functions of fluctuations below,

$$\lambda_{mm}(t) = N\left[\frac{\langle m(t)^2 \rangle}{\langle m(t) \rangle^2} - 1\right] \sim t^{\lambda_{mm}}, \tag{4.4}$$

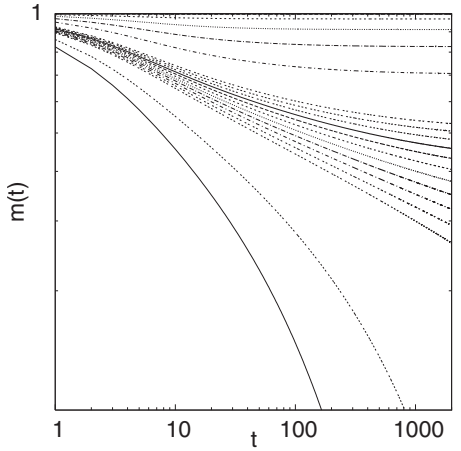

FIG. 15. The relaxation of magnetization $m(t)$ for the six-states GG model in three dimensions in double-log plot. For temperatures in $0.3 \leq T \leq 1.0$, the data are plotted with an interval of $\Delta T=0.1$ and so do in $0.7 \leq T \leq 0.8$ with $\Delta T=0.01$.

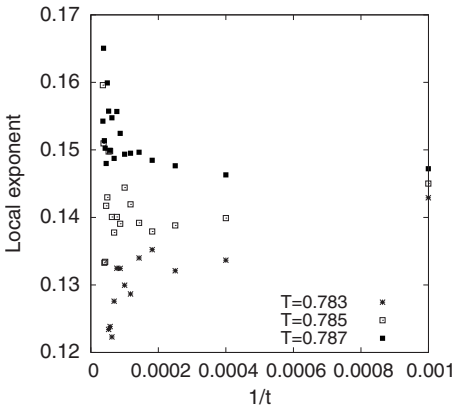

FIG. 16. The behavior of the local exponent $\lambda(t)$ for the six-states GG model in three dimensions is plotted for $T=0.783, 0.785, 0.787$.

$$\lambda_{me}(t) = N\left[\frac{\langle m(t)e(t)\rangle}{\langle m(t)\rangle\langle e(t)\rangle} - 1\right] \sim t^{\lambda_{me}}, \tag{4.5}$$

which are convenient for the estimation of individual exponents, where $e(t)$ is the energy per site at time t. Following the local exponent for the order parameter in Eq. (4.2), it is convenient to define local exponents for NER functions of fluctuations [32]

$$\lambda_{mm}(t) = \frac{d \log f_{mm}(t)}{d \log t}, \tag{4.6}$$

$$\lambda_{me}(t) = \frac{d \log f_{me}(t)}{d \log t}. \tag{4.7}$$

The dynamical exponents are also expressed as

$$\lambda_{mm} = \frac{d}{z}, \tag{4.8}$$

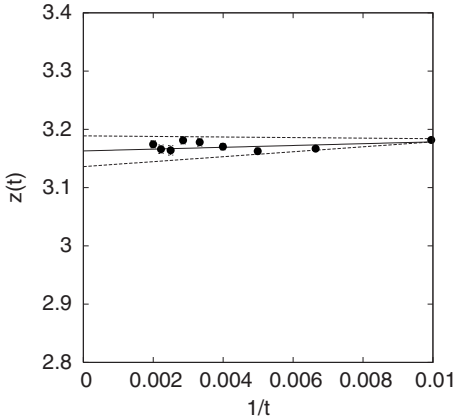

FIG. 17. Local exponent $z(t)$ for the six-states GG model in three dimensions. $T_c=0.785$ is assumed.

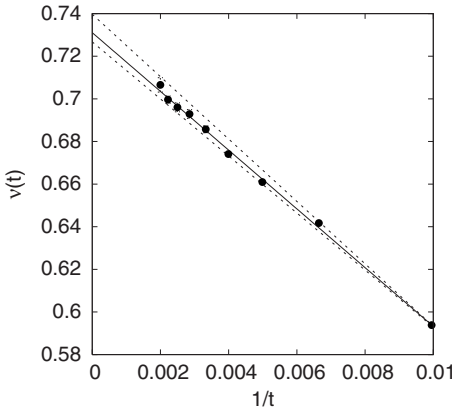

FIG. 18. Local exponent $\nu(t)$.

$$\lambda_{me} = \frac{1}{z\nu}. \tag{4.9}$$

The dynamical exponent λ_m which characterizes the power-law decay of the magnetization at the critical point is expressed as

$$\lambda_m = \frac{\beta}{z\nu}. \tag{4.10}$$

The local exponents corresponding to relations (4.8), (4.9), and (4.10) are defined as

$$z(t) = \frac{d}{\lambda_{mm}(t)}, \tag{4.11}$$

$$\nu(t) = \frac{\lambda_{mm}}{d\lambda_{me}(t)}, \tag{4.12}$$

$$\beta(t) = \frac{\lambda_m(t)}{\lambda_{me}(t)}, \tag{4.13}$$

by which one can estimate each exponent directly from a plot versus $1/t$ like Fig. 16. The results are shown in Figs. 17–19. Estimating the values for $t\to\infty$, i.e., $1/t=0$, we obtain $z=3.163$, $\nu=0.731$, and $\beta=0.321$ from each figure.

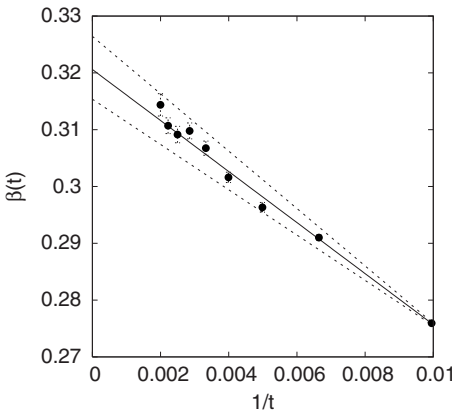

FIG. 19. Local exponent $\beta(t)$.

TABLE III. Summary of estimated transition temperatures T_c, local exponent λ and critical exponents z, ν, and β for GG models in three dimensions.

q	T_c	λ	z	ν	β
6	0.785(2)	0.137(6)	3.16(3)	0.731(8)	0.321(6)
8	0.783(2)	0.136(10)	3.16(3)	0.731(8)	0.316(5)
⋯					
16	0.783(2)	0.135(10)	3.17(2)	0.731 (5)	0.318(4)
⋯					
∞	0.783(1)	0.134(7)	3.17(2)	0.729 (3)	0.317(2)

The same analysis is made for other q cases. The results are summarized in Table III. We found that the spin discreteness is irrelevant, and the transition belongs to the same universality class as in the (continuous) XY case in spite of the discrete energy spectrum. This is the same behavior as mentioned in the pure case [31].

V. REMARKS

We have performed the NER analysis of KT transition for the q-state clock GG model with $q=6$, 8, 10, 12, 14, 16, and 1024 in two dimensions. Since the successive transitions of FM-KT-PM type are expected as in the pure clock model, two kinds of scaling plot are applied to distinguish them. The results are summarized in Table I for the Villain-type and in Table II for the cosine-type. For both models, it is found that the same type of successive transitions and almost the same upper critical temperature as in the continuous case are observed for all cases. The lower transition temperatures T_{KT2} are linear in $1/q^2$. This indicates that the behavior is the same as in the pure case, and the phase diagram is like in Fig. 1 as expected. The results for the Villain-type model are consistent with the duality relation (2.6) [30] in the present accuracy. Similar behaviors are observed for the cosine type, while the model is not self-dual. This would be investigated in the future.

We have also performed the NER analysis of second-order transition and critical exponents for the q-state clock GG model with $q=6$, 8, 16, and 1024 in three dimensions. The results are summarized in Table III. It is found that the spin discreteness is irrelevant, and the transition belongs to the same universality class as in the (continuous) XY case.

ACKNOWLEDGMENTS

This work is supported by a Grant-in-Aid for Scientific Research Program (Grant No. 19540397) from the Ministry of Education, Culture, Sports, Science and Technology of Japan. The authors also thank the Supercomputer Center, Institute for Solid State Physics, University of Tokyo for the facilities and the use of the SGI 3700.

[1] M. Rubinstein, B. Shraiman, and D. R. Nelson, Phys. Rev. B **27**, 1800 (1983).
[2] E. Granato and J. M. Kosterlitz, Phys. Rev. B **33**, 6533 (1986).
[3] J. M. Kosterlitz and D. J. Thouless, J. Phys. C **6**, 1181 (1973).
[4] M. G. Forrester, H. J. Lee, M. Tinkham, and C. J. Lobb, Phys. Rev. B **37**, 5966 (1988).
[5] A. Chakrabarti and C. Dasgupta, Phys. Rev. B **37**, 7557 (1988).
[6] M. G. Forrester, S. P. Benz, and C. J. Lobb, Phys. Rev. B **41**, 8749 (1990).
[7] M. Paczuski and M. Kardar, Phys. Rev. B **43**, 8331 (1991).
[8] M. J. P. Gingras and E. S. Sørensen, Phys. Rev. B **46**, 3441 (1992).
[9] T. Nattermann, S. Scheidl, S. E. Korshunov, and M. S. Li, J. Phys. (Paris), Colloq. **5**, 565 (1995).
[10] M. C. Cha and H. A. Fertig, Phys. Rev. Lett. **74**, 4867 (1995).
[11] G. S. Jeon, S. Kim, and M. Y. Choi, Phys. Rev. B **51**, 16211 (1995).
[12] L. H. Tang, Phys. Rev. B **54**, 3350 (1996).
[13] S. Scheidl, Phys. Rev. B **55**, 457 (1997).
[14] J. M. Kosterlitz and M. V. Simkin, Phys. Rev. Lett. **79**, 1098 (1997).
[15] J. Maucourt and D. R. Grempel, Phys. Rev. B **56**, 2572 (1997).
[16] S. E. Korshunov, Phys. Rev. B **48**, 1124 (1993).
[17] C. Mudry and X. G. Wen, Nucl. Phys. B **549**, 613 (1999).
[18] Y. Ozeki and H. Nishimori, J. Phys. A **26**, 3399 (1993).
[19] Y. Ozeki, J. Phys. A **36**, 2673 (2003).
[20] D. A. Huse and H. S. Seung, Phys. Rev. B **42**, 1059 (1990).
[21] J. Maucourt and D. R. Grempel, Phys. Rev. B **58**, 2654 (1998).
[22] T. Olson and A. P. Young, Phys. Rev. B **61**, 12467 (2000).
[23] N. Akino and J. M. Kosterlitz, Phys. Rev. B **66**, 054536 (2002).
[24] M. J. P. Gingras, Phys. Rev. B **44**, 7139 (1991).
[25] M. Cieplak, J. R. Banavar, M. S. Li, and A. Khurana, Phys. Rev. B **45**, 786 (1992).
[26] R. H. Koch, V. Foglietti, W. J. Gallagher, G. Koren, A. Gupta, and M. P. A. Fisher, Phys. Rev. Lett. **63**, 1511 (1989).
[27] P. L. Gammel, L. F. Schneemeyer, and D. J. Bishop, Phys. Rev. Lett. **66**, 953 (1991).
[28] C. Dekker, W. Eidelloth, and R. H. Koch, Phys. Rev. Lett. **68**, 3347 (1992).
[29] J. V. José, L. P. Kadanoff, S. Kirkpatrick, and D. R. Nelson, Phys. Rev. B **16**, 1217 (1977).
[30] K. Takeda, T. Sasamoto, and H. Nishimori, J. Phys. A **38**, 3751 (2005).
[31] M. Oshikawa, Phys. Rev. B **61**, 3430 (2000).
[32] Y. Ozeki and N. Ito, J. Phys. A: Math. Theor. **40**, R149 (2007).
[33] N. Ito, Physica A **192**, 604 (1993); **196**, 591 (1993).
[34] N. Ito, K. Hukushima, K. Ogawa, and Y. Ozeki, J. Phys. Soc. Jpn. **69**, 1931 (2000).
[35] Y. Ozeki, N. Ito, and K. Ogawa, Supercomputer Center, ISSP, University of Tokyo Activity Report No. 1999, 2000,

pp. 37–51.
[36] Y. Ozeki and N. Ito, J. Phys. A **31**, 5451 (1998); N. Ito, Y. Ozeki, and H. Kitatani, J. Phys. Soc. Jpn. **68**, 803 (1999); K. Ogawa and Y. Ozeki, *ibid.* **69**, 2808 (2000); Y. Ozeki and N. Ito, Phys. Rev. B **64**, 024416 (2001); Y. Ozeki, N. Ito, and K. Ogawa, J. Phys. Soc. Jpn. **70**, 3471 (2001).
[37] H. J. Luo, L. Schülke, and B. Zheng, Phys. Rev. Lett. **81**, 180 (1998); Phys. Rev. E **57**, 1327 (1998).
[38] Y. Ozeki, K. Ogawa, and N. Ito, Phys. Rev. E **67**, 026702 (2003); Y. Ozeki and N. Ito, Phys. Rev. B **68**, 054414 (2003).
[39] Y. Ozeki, K. Kasono, N. Ito, and S. Miyashita, Physica A **321**, 271 (2003).
[40] Y. Ozeki and K. Ogawa, Phys. Rev. B **71**, 220407(R) (2005).
[41] J. Villain, J. Phys. (Paris) **36**, 581 (1975).
[42] H. Nishimori, Prog. Theor. Phys. **66**, 1169 (1981).
[43] Y. Ozeki and H. Nishimori, J. Phys. A **26**, 3399 (1993).
[44] In the skew boundary condition, the boundary spins in the x or y directions are connected to those on the next layer, and the boundary spins in the z direction are connected periodically.
[45] J. M. Kosterlitz, J. Phys. C **7**, 1046 (1974).
[46] We find a modification in the estimation of the transition temperature for the continuous case in the Villain-type model [$T_{\mathrm{KT1}}=0.429(10)$] from the previous one [40]. This comes from longer-step observations with higher resolution for sampling temperatures.
[47] Precisely speaking, a modification scheme has proposed for the duality theory in some random systems [48], which provides transition points shifted slightly from the original results. In the accuracy of present results, such deviation cannot be detected numerically. Thus, we say "applicability" here.
[48] M. Ohzeki, Ph.D. thesis, Tokyo Institute of Technology, 2008.